

## 11 Electron Beam Diagnostics

### *Synopsis*

The FERMI beam diagnostics includes a complete set of instruments specifically designed to completely characterize the FERMI free electron beams. Measurements to be performed at different machine sections are presented, starting from the photo-injector and moving downstream, through the linac and the FEL.

The characterization of the photo-injector, given the electron bunch physical properties, is based on a set of traditional instruments. The bunch charge and the transverse and longitudinal profiles are measured by means of a current transformer, movable Faraday cups, Yttrium Aluminium Garnet Cerium crystal (YAG:Ce) screens and a Cherenkov radiator coupled to a single sweep streak camera respectively. This set-up ensures a detailed characterization of the bunch non-gaussian longitudinal profile, one of the new features of the FERMI photo-injector. A movable slit plus screen assembly measures the emittance of the space charge dominated, low energy bunch, while a dispersive beamline is foreseen for energy, energy spread and longitudinal phase space measurements. The uncorrelated energy spread can also be measured exploiting the bunch correlation between energy and longitudinal position.

The following linac sections are equipped with standard intra-section diagnostics stations (X-Y position, profile and charge). Two cavity beam position monitors (BPMs) with micrometer resolution measure the bunch transverse position at the entrance of the first ELETTRA type accelerating section (S1) for beam centering.

Two four-screens stations separated in betatron phase by  $\pi/4$  are located downstream from BC1 and at the end of the linac respectively, and used to accurately measure the beam emittance.

Dedicated diagnostic stations also equip both bunch compressors (BC1 and BC2): the bunch length, arrival time (i.e. jitter) with respect to the reference, energy and energy spread are measured non-destructively enabling on-line monitoring of the beam. Measurements of the coherent radiation (CSR, CDR) generated by short bunches in the compressors provide relative bunch length information. A newly developed bunch arrival time monitor based on an electro-optical technique performs bunch arrival time measurements.

Finally a dedicated "energy BPM" is located in the dispersive section of each chicane to monitor the beam energy. The beam energy spread is crosschecked (destructively) either using a wire scanner or a screen. Two radio frequency deflectors, located downstream from BC1 and at the end of the linac respectively, are needed to accurately measure bunch length and, coupled to a downstream dipole, to measure slice emittances and slice energy spread.

A set of three cavity BPMs is placed in a drift space, in front of both the FEL1 and the FEL2 modulator undulators, to measure the beam transverse position with micron accuracy in the single shot mode and to check the beam alignment in the transverse (X-Y) coordinate plane. An electro-optical sampling station provides single shot measurements of the bunch arrival time and of the longitudinal profile non-destructively.

Finally, intra-undulator diagnostics stations, measuring the transverse beam position and the FEL photon beam intensity, are used to optimize the FEL process.

## 11.1 Introduction

The chapter has two parts: in the first (Paragraphs: 11.1 to 11.2.11) the beam parameters to be measured are listed following the machine topology, from the photo injector down to the FEL sections. The second part (Paragraph: 11.3) covers the instruments foreseen to meet the diagnostics specifications.

Some instruments, such as those to measure the bunch length and arrival time with  $< 100$  fs resolution, require a significant development effort. In particular, the bunch arrival time is measured at several locations using a novel electro-optical technique that has demonstrated sub-100 fs resolution.

On-line energy and energy spread monitoring is another demanding task; in the bunch compressor region a single instrument able to cover the full operating range while preserving state of art performance is still being developed.

For the radio frequency deflectors, innovative approaches are under investigation to add additional features to those of the basic set-up. In particular, a two-plane RF deflector is foreseen, able to handle full energy beams.

The quality of the photoinjector high brightness electron beam plays a crucial role for the performance of the FERMI seeded FEL. Optimization of the gun is made possible by a complete set of beam monitors for an extensive characterization of the 5 MeV electron beam longitudinal and transverse phase space.

A set of standard instruments for measuring the transverse position and the charge per bunch is installed in each gap between linac sections to ensure non intercepting, on-line beam monitoring. Both the BC1

and the BC2 bunch compressors (*see par.* 11.2.5) are completely instrumented to provide signals to beam energy and bunch length stabilization feed-back systems.

In a seeded FEL like FERMI the temporal and spatial overlap between the electron beam and the seed laser pulse has to be checked, particularly at the input of the modulator; this is obtained using a pair of dedicated cavity BPMs associated with an electro-optical sampling station. The onset of laser induced bunching is checked downstream from the modulator chicane by coherent transition radiation based diagnostics. The FEL radiation intensity is monitored along the radiator chain, by means of suitable optical detectors, all the way through saturation. Finally, the complete spectral-angular distribution is measured by dedicated spectrometers, one for each FEL chain.

Standard beam line diagnostics is presented briefly, while state-of-the-art diagnostics is discussed in more detail.

## 11.2 Measurements to be Performed

### 11.2.1 Injector Diagnostics

The injector is equipped with a full complement of instruments to measure the electron beam properties, in order to produce input signals for the machine protection system and information vital for understanding the FEL lasing process. Considerations about the photoinjector beam instrumentation and diagnostics are also found in section 5.5.

The key electron beam parameters monitored along the injector section are discussed below. Of these, only the bunch charge and the transverse beam position can be measured with non-intercepting devices.

The primary purpose of beam position and profile monitors is to help align the beam on axis through the first accelerating cavity. The beam rms diameter ranges from 0.5 to 2 mm and is measured with an accuracy of 10 – 100  $\mu\text{m}$ , depending on the type of monitor used and on beamline parameters at the monitor. Position and profile measurements also provide information on the laser beam stability.

At low energies, where the beam dynamics is strongly dominated by space charge effects, accurate emittance measurements are performed using either a 2D pepper-pot device or a 1D slit array, as described in Section 11.3.7. The thermal emittance, whose expected value is  $\sim 0.6$  mm mrad, is measured at low bunch charge ( $\sim 50$  pC) using the solenoid plus scintillation screen technique [1]. Beam charge measurements aimed at providing information on possible drifts of the photocathode quantum efficiency and at helping to adjust the laser settings, in particular the correct phase between the laser and RF gun, are performed using Faraday cups (*see par.* 11.3.10.1) and/or a current transformer (*see par.* 11.3.10.2).

The nominal bunch charge varies between 0.3 nC and 1.0 nC and is measured with 10 - 50 pC resolution depending on the type of monitor used and on the beam parameters at the monitor.

In order to check the beam proper alignment and to optimize the collimation efficiency, additional measurements are implemented on the photoinjector laser beam.

The electron beam longitudinal current distribution and the bunch length are measured using an aerogel Cherenkov emitter coupled to a streak camera (*see Par.* 11.3.16). The expected bunch length of about 10 ps is measured with 200 fs resolution.

A magnetic spectrometer is a crucial diagnostics element for establishing the proper RF gun tune and overall performance. The dispersive beamline provides information on the beam energy, energy spread and longitudinal phase space. The expected rms energy spread varies in the range 100 – 300 keV depending on the phase between the laser pulse and the gun peak field. The design goal is to measure it with 1 % resolution.

A compact optical bench, located in the tunnel close to the gun, is dedicated to the photocathode laser diagnostics and used to monitor the laser performance on-line, based on the “*virtual cathode*” scheme (see Par. 5.5.2.1).

### 11.2.2 Laser Heater Diagnostics

The laser heater design is based on a four magnet chicane with a short undulator in between the second and the third dipole (see Par. 6.2.1). The laser heater diagnostics will be mainly dedicated to the alignment of the electron beam in the undulator and to guaranteeing the transverse overlap of the electron beam with the laser beam. Two stripline BPM (section 11.3.3) plus YAG:Ce screen pairs (Section 11.3.5) are installed upstream and downstream from the undulator respectively. The BPM will measure the electron beam position with a resolution of ~50 microns while the YAG:Ce will be used to measure the electron beam and laser beam profiles.

### 11.2.3 Linac1, Linac2, Linac3 and Linac4

The accelerating structures of the linacs (1, 2, 3 and 4) are equipped with intra section diagnostics, where transverse position and profile along with the bunch integrated charge are measured. The main purpose of the intra section diagnostics is to ensure the correct steering of the beam on the axis of the accelerating structures while monitoring the efficiency of the charge transport process. BPMs and current transformers provide this functionality, non destructively. Screens have been adopted for “first trajectory” steering and for beam profile measurements. Due to longitudinal space constraints ad-hoc instruments have been conceived, deeply integrated in the machine layout. Precise initial alignment is of fundamental importance to provide the beam position relative to the accelerating structures.

### 11.2.4 X-Band Linearizer

The X-band linearizer is necessary to longitudinally manipulate the electron bunch. It is operated at 11.423996 GHz, the 4th harmonic of the accelerating S-band frequency. Two dedicated BPMs are used to monitor the bunch trajectory in order to keep it aligned on the cavity axis. A wide band (BW > 10 GHz) electromagnetic pick-up, connected to a multi channel, wide band (BW = 15 GHz), real-time (not sampling) oscilloscope, will provide information on the relative bunch phase with respect to the X-band frequency.

### 11.2.5 BC1 and BC2 Compressors Diagnostics

Bunch compressors (BC) are key components of the seeded FEL. A complete set of non intercepting diagnostics is foreseen to produce error signals for the feedback loops used to stabilize the electron bunch energy and peak current [2]. The different operation regimes foreseen for FERMI call for a flexible set-up of both the bunch compressors and the associated diagnostics. To this end beam position monitors in dispersive regions (called “energy BPMs” or EBPMs, see Section 11.3.4) and diagnostics

stations containing an optical transition radiation (OTR) screen (Section 11.3.6) and a wire scanner (Section 11.3.9) are mounted inside the bunch compressors to measure the beam position, energy and energy spread. In particular EBPMs will be used for the on-line, non-intercepting energy measurements driving the energy feedback. A relative bunch length monitor is needed to find the optimum compression value and to stabilize the bunch peak current. It will be based on the detection of coherent synchrotron radiation (CSR) from the last bend of the BCs and of coherent diffraction radiation (CDR) generated from a downstream the same bend. The system allows non-intercepting measurement of the relative bunch length. The bunch arrival time at the entrance and at the exit of the compressor will be measured shot by shot using a bunch phase monitor (Section 11.3.15).

A schematic layout of the full complement of bunch compressor diagnostics is shown in Figure 11.2.1.

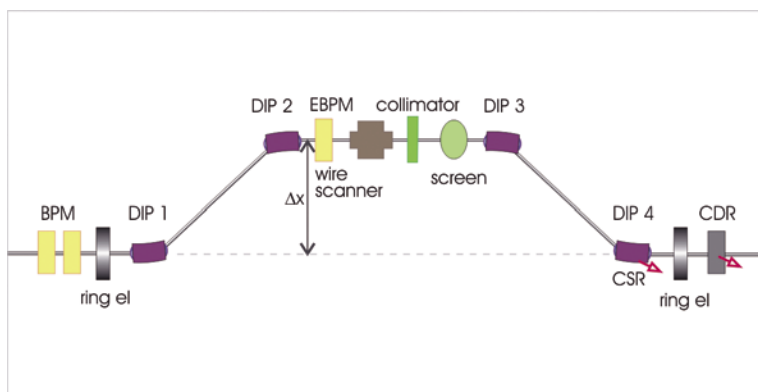


**Figure 11.2.1:**  
Bunch Compressor Diagnostics layout.

### 11.2.6 Front-end Last Diagnostics Station

A diagnostics station will be located immediately downstream from the second bunch compressor (BC1), just before the beam dump. It will mainly consist of two sub-systems: a RF deflector, called “low energy deflector”, plus a multi-screen emittance measurement station. The RF deflector (described in 11.3.12) is a vertically deflecting, compact (~1 m), 5 cell standing wave structure used to measure both the longitudinal profile and the horizontal slice emittance.

The multi-screen station is used to measure the beam transverse emittance and investigate the effects of CSR induced emittance dilution.

The energy and energy spread will be measured by a YAG:Ce screen located after the beam dump bending magnet.

### 11.2.7 End of Linac and Spreader Diagnostics

The linac end has been identified as another key location for beam diagnostics. A high energy RF deflector, a multi-screen emittance station and a spectrometer will be located in this area.

The RF deflector (described in 11.3.12) is a traveling wave structure,  $\sim 2$  m long, powered by a dedicated modulator. It does allow for both vertical and horizontal deflections. This feature will make it a unique instrument that allows measuring both the vertical and the horizontal slice emittance using a YAG:Ce screen placed 10 m downstream from the deflector. Furthermore, on a second screen downstream from the electron beam dump bending magnet, the correlated slice energy spread can be measured.

Four screens properly spaced in phase are also mounted in the same area to measure the beam emittance. Both the vertical and the horizontal beta function values at the screens are 5 m, producing a  $56 \mu\text{m rms}$  beam size for a  $1 \text{ mm mrad}$  normalized emittance. The optical detection system resolution is specified to be  $10 \mu\text{m}$ . Screens behind the dump bending magnet allow it to function as a spectrometer.

A collimator, located in a high dispersion region of the spreader, will provide energy collimation to meet undulator radiation protection and beam dynamics requirements. A BPM and a screen are foreseen both in front and behind the collimator for transverse profile and position measurements. Collimator blades with micrometer positioning resolution are expected to be sufficient for both betatron space and energy cleaning. Energy and energy spread measurement systems will also be provided downstream from the collimator.

### 11.2.8 FEL Modulator Diagnostics

Because the interaction of the seed laser with the electron beam takes place in the FEL modulator, the beam position and angle at the modulator entrance is highly critical. A pair of high resolution cavity BPMs is therefore installed in front of it (see Par. 11).

The superposition in space of the seed laser beam and the electron beam will be checked by means of YAG:Ce screens (Section 11.3.5) placed both upstream and downstream from the modulator while their superposition in time will be checked by an Electro-Optical Sampling station (EOS) (see Par. 11.13.9) located upstream. The EOS will provide single shot, non-intercepting measurements of the bunch longitudinal profile, its arrival time and its jitter.

### 11.2.9 FEL Radiator Diagnostics

The FEL modulator is followed by a chicane which converts beam energy modulation into current modulation. The desired laser induced microbunching will be measured by detecting the coherent transition radiation (CTR) produced by the beam in traversing a thin pop-in screen. A pop-in diagnostic station similar to the ones installed in between undulator sections (see Par. 1.13.3), is located immediately downstream from the chicane and just in front of the first undulator section, and serves the purpose. The intensity of the CTR will be measured by a silicon photodiode. For FEL-1, the radiation can be transported out of the vacuum chamber and its spectrum measured using a UV spectrometer since it is mainly emitted at the seed laser wavelength in the near UV. For FEL-2, because the CTR wavelength is shorter than  $\sim 100 \text{ nm}$  (vacuum UV), transport in air is not possible and an in-vacuum solution is foreseen.



Another crucial parameter to be measured at the modulator location is the beam position: a cavity BPM placed downstream from the pop-in station is provided for this purpose. The beam profile will be measured using either a YAG:Ce or an OTR screen. Multipurpose diagnostics stations are also foreseen along the FEL undulator chain, one at each straight section in between undulator sections; their configuration and working principle are described in Paragraph 11.3.8.

Additional parameters to be measured along the beam trajectory are: the electron and photon beam relative position, their profile, their intensity and the induced bunching evolution. This set of measurements will be done using the same kind of tools described above but, because the photon and the electron beams now overlap, in a more complex configuration.

### 11.2.10 Beam Dump and FEL Downstream End Diagnostics

Both the FEL and the spontaneous radiation produced in the radiator must be characterised in terms of energy per pulse, transverse profile and divergence, pointing stability and spectral distribution.

The FEL radiation beam transverse profile and pointing stability will be measured by ad hoc developed screens since the beam energy density could cause damage. Information on the spontaneous radiation spectral distribution, important for the undulator final tuning procedure, as well as on FEL radiation will be obtained by measuring the radiation spectral distribution on-axis and its angular distribution. As an example, the K factor of each undulator section can be tuned by optimizing the frequency of the on axis first harmonic. Most of these measurements, including the spectral distribution, will be done in single shot, using the diffracted beam from monochromators in the experimental hall (see Par. 8.4.3). The FEL energy and intensity stability will be measured in a gas cell system (see Par. 8.3.1).

In order to measure the electron beam final timing jitter a station equipped with a synchro-scan streak camera detects the visible radiation extracted from the last beam dump magnet. The device is illuminated simultaneously by SR and by a reference optical pulse from the ultra stable timing system or by the user laser. In spite of a nominal resolution of less than  $2 p_{FWHM}^S$  this technique provides the relative time stability of the electron bunch with respect to an optical reference pulse (or a user laser pulse) with a sensitivity of the order of 400 fs.

## 11.3 Instrumentation

### 11.3.1 Beam Position Monitors

Three different kinds of beam position monitors will be used. Matched stripline BPMs are foreseen where high resolution is not required while cavity BPMs are used where high resolution is needed, like at the entrance of the FEL modulator.

### 11.3.2 Cavity Beam Position Monitor

Cavity beam position monitors (TM<sub>110</sub> cavity type) are foreseen where resolution of the order of 1  $\mu\text{m}$  is required (not achievable with matched stripline BPMs). Beam based alignment will heavily rely on their performance. In particular, cavity BPMs are used in front of the modulator (2 cavity BPMs in a drift) to accurately measure the transverse position and angle of the beam entering the modulator. Accurate measurements of the beam transverse position are also needed in between undulator sections.

The present design is, conceptually, a scaling from X-band to C-band of the cavity BPM developed for NLC [3]. The complete design study is reported in ref. [4], while in Figure 11.3.1 are summarized the parameters and a 3D model of the BPM is shown. Analytical and numerical models show that the resolution at C-band remains below  $1\ \mu\text{m}$ . Furthermore, common mode losses of the scaled object are at the same level as those of the original X-band device.

Careful mechanical implementation and integration with other intra-section diagnostics is needed to guarantee not only resolution and long term stability but also accurate and reproducible alignment.

C-band cavity BPM	
Cavity gap	10mm
Cavity radius	26.4mm
Beam pipe radius	10mm
Coupling WG	$34.85 \times 6\text{mm}^2$
Distance WG to beam axis	12mm
WG standard	WR137
Resonant frequency	6.5GHz
Unloaded Q factor	8530
External Q	10500
Coupling coefficient	0.1
Reference cavity	
Cavity gap	10mm
Cavity radius	17.6mm

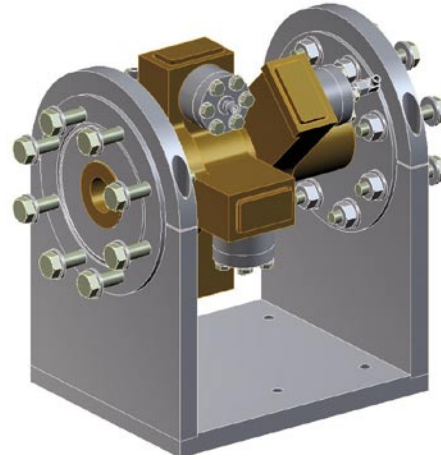


Figure 11.3.1: Dimensional and RF parameters of the C-band cavity BPM and the reference cavity (left). C-band cavity BPM 3D model with its four coupling waveguides and reference cavity (right).

### 11.3.3 Stripline Beam Position Monitors

Most of FERMI BPMs located where space is not a stringent constraint, like in between linac sections, are matched stripline BPMs. The strips are 150 mm long and signal detection is based on commercial, 500 MHz electronics. Sum signals also provide fast beam loss information during tune up. The strips are fixed to and aligned with respect to flanges which are, in turn, fixed to the BPM body. The mechanical uncertainty on the centre of the assembly position is specified to be less than  $20\ \mu\text{m}$ . The readout electronics is designed so that, after careful initial alignment to  $50\ \mu\text{m}$  rms absolute accuracy, the long term (8 hours) single shot absolute position peak to peak fluctuation remains smaller than  $\sim 70\ \mu\text{m}$ .

For locations where longitudinal space is an issue, like in the photoinjector, resonant striplines [5], [6], less bulky than matched ones, are being considered; preliminary tests indicate that they provide a resolution approaching that of cavity beam position monitors. The dedicated electronics needs further developing.



### 11.3.4 Energy Beam Position Monitors

The beam centroid transversal displacement in the BC1 and BC2 bunch compressors,  $\Delta x$ , spans over  $\sim 100$  mm. A vacuum chamber at least 150 mm wide would therefore be needed to accommodate the electron beam ( $\pm 3\sigma = 35$  mm) plus the closed orbit allowance. On the other hand, the rms energy stability required by the FEL ( $\Delta E/E=0.1\%$ ) does translate, in terms of rms displacement variations, into 200  $\mu\text{m}$  under nominal BC1 operating conditions. To correctly operate the feedback system the resolution of the position measurement must be at least four times better. A single shot resolution of  $\sim 50$   $\mu\text{m}$  is needed, a specification that can not be met with a chamber much wider than 60 mm. In order to accommodate the up to 100 mm beam displacement in the bunch compressor, the central (2<sup>nd</sup> and 3<sup>rd</sup>) dipoles and the BPMs will therefore be mounted on high reproducibility translators and moved, to follow the beam displacement, which allows reducing the chamber width to 60 mm only. Further design studies and simulations are in progress.

Other position diagnostics options, such as the one proposed at DESY [7], based on the measurement of the relative time difference between two pulses generated in a transverse strip-line arrangement, are also under consideration.

### 11.3.5 Scintillation Screens

Screens, either scintillators or the optical transition radiators (OTR, described in section 11.3.6), are used to measure the electron beam transverse profile. In particular, YAG:Ce screens with thickness of about 100  $\mu\text{m}$  are used in the photoinjector. Thin YAG:Ce is a fast scintillator with excellent mechanical and chemical resistance. YAG:Ce screens are made from selected inorganic crystal materials with cubic structure; the grain size and transparency ensure a spatial resolution better than 10  $\mu\text{m}$ , compatible with 10  $\mu\text{m}$  limit of the CCD sensor and optical setup. The material mechanical properties allow producing thin screens, down to 0.005 mm thick. The wavelength of maximum emission is 550 nm, the decay constant 70 ns and the photon yield at 300 K 35000 photons/MeV [8]. Screen positions along the beamline are chosen to avoid saturation effects at high charge densities ( $\sim 0.1\text{pC}/\mu\text{m}^2$ ). YAG:Ce screens can also be used to detect photon beams, from VUV to gamma rays.

YAG:Ce screens are the preferred solution at low energy because of their higher photon yield compared to OTR screens. Standard ceramic scintillating materials such as Aluminium Oxide doped with  $\text{Cr}_2\text{O}_3$  (commercially called Chromox) have been discarded because of their poorer performance in terms of spatial resolution, decay time and afterglow. Screens will also be used during laser alignment of accelerator components.

### 11.3.6 Optical Transition Radiation (OTR) Screens

OTR screens are usually thin metal foils or metal coated substrates. The choice of the metal depends on the application but most often Ti, Al and Ag are used. The substrates can be mylar Teflon or Si. Because OTR is a local, surface, instantaneous effect and since very thin foils can be used, it provides spatial resolutions down to  $\sim 1$   $\mu\text{m}$ , high linearity and high radiation resistance. The instantaneous OTR emission can thus be used to measure the longitudinal beam profile. Such screens are also used as CTR emitters for micro bunching detection, as previously discussed. At present we are considering to use 0.3 mm Si substrates coated with 200 nm of Al. The photon yield becomes comparable to that of the YAG:Ce screen one only at a few hundred MeV.

### 11.3.7 Emittance Measuring Devices

The emittance measurement at low energy (5 MeV) will be based on single slit and multi-slit (pepper-pot) devices which slice-up the beam into well separated sampling beamlets by means of an intercepting mask. The slits convert the space charge dominated incoming beam into several emittance dominated beamlets which then drift to a detection screen. Slit spacing has to be larger than the slit width and smaller than the beam size to ensure that the image can be resolved [9]. The drift space in between the mask and the screen must be long enough in order to have high resolution for low emittance beams and short enough to prevent overlapping of beamlet profiles on the screen. Evaluation of the rms emittance only depends on the slit mask geometry, the beamlets size and the intensity distribution on the screen [10], the resolution being mainly limited by jitters of the beam transverse position or profile.

### 11.3.8 Intra-Undulator Pop-in Station

Multipurpose pop-in stations are compact devices equipped with several screens. (see Figure 11.3.2). They are meant to provide information on the electron and photon beam transverse position. Each pop-in will consist of a remotely movable holder mounted at 45° with respect to the accelerator axis and holding at least three elements: a YAG:Ce screen, an OTR screen and a UV mirror. The system is interceptive and therefore only used during commissioning and for periodic checks.

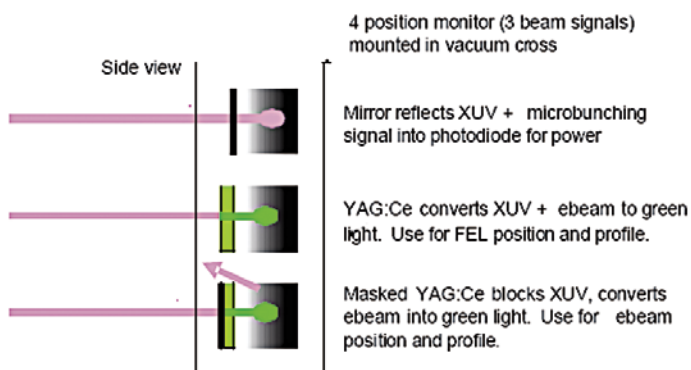


Figure 11.3.2:  
Multi screen functional scheme.

Visible light from the YAG:Ce screen will be used to image both the XUV photon beam and the electron beam with a CCD camera. It provides information about both the electron and the XUV beams position and profile. A mask can also be used to block the XUV radiation and allow only the electron beam to reach the YAG:Ce screen.

The OTR screen is used to image the electron beam only, since FEL radiation reflected by the screen is stopped by the vacuum viewport. XUV radiation can be detected by a Si photodiode, to provide an absolute energy measurement and thus reconstruct the gain curve of the FEL along the undulator chain.

The CTR signal due to laser induced bunching can also be measured on the same detector. To discriminate between the two signals a filter can be used, since the CTR signal does appear at the seed laser wavelength. This part of the equipment needs to be in ultra high vacuum, to avoid XUV radiation absorption in air. Possible screen radiation damage problems by the high peak power XUV beam need further investigation.

### 11.3.9 Wire-Scanners

Compared to screens, wire scanners can provide resolution down to 1  $\mu\text{m}$  level, dominated by the wire diameter. On the other hand they are delicate, comparatively slow and therefore able to reconstruct a beam profile only on a multi shot basis.

### 11.3.10 Bunch Charge Measurement

#### 11.3.10.1 Faraday Cup

A Faraday cup with better than 10 pC accuracy is used to measure the absolute bunch charge and to calibrate non-intercepting charge measuring instruments such as BPMs or integrating current transformers. It also serves as beam dump for the injector beam.

#### 11.3.10.2 Integrating Current Transformers

Integrating Current Transformers (ICT) are used to measure non-destructively the beam charge with high relative accuracy. Commercial ICTs will be used that integrate the signal with a time constant of the order of 10 nsec, depending on the model. They are embedded in conflat flanges for direct mounting on the beam pipe [11]. The latter feature is crucial when space is limited, like in the photoinjector.

### 11.3.11 Energy Spectrometers

#### 11.3.11.1 Photo-injector Energy Spectrometer

A first design based on a 90° bending magnet followed by a YAG:Ce screen has been studied and is described in Chapter 5. The intrinsic relative energy resolution is  $\delta_{\text{min}} \geq 2/D \sim 2 \text{ keV}$ , where D is the dispersion value at the screen. Alternative solutions with smaller bending angles are being evaluated both in terms of energy resolution and of mechanical constraints.

#### 11.3.11.2 BC1 Energy Spectrometer

A bending magnet will be located downstream from BC1 and used as an energy spectrometer. An energy resolution of the order of 60 KeV is the design value.

#### 11.3.11.3 Linac-end Energy Spectrometer

An energy and energy spread measurement will be performed at the end of the linac. It will make use of the existing linac transfer line bending magnets that will be used for FERMI as beam dump magnets. The energy stability requirements of FEL are of  $\delta E/E = (\pm 0.5 \times 10^{-4})$ . The design relative resolution of the spectrometer has been chosen to be  $2.5 \times 10^{-5}$  which means at 1.2 GeV, an absolute resolution of 30 keV. The dispersion provided by the two bending magnets and the drift space between them is  $D_{\text{tot}} = 1.85 \text{ m}$ . The energy resolution translates directly into a space resolution of 46  $\mu\text{m}$ . The relative energy spread,

expected to be 0.01%-0.1%, will be measured with a resolution of 5%. The energy spread in combination with the dispersion ( $D_{\text{tot}}=1.85$  m) will induce a transverse broadening of the beam, whose expected rms beam size is  $185 \mu\text{m}$ . The 5% resolution requirement translates then to  $9 \mu\text{m}$  spatial resolution. The resolution requirements for both beam energy and energy spread measurements should be met using OTR screen and high resolution optics systems of the same kind of those used for emittance measurements.

### 11.3.12 Radio Frequency Deflectors

Two radiofrequency deflectors are foreseen as diagnostic tools, one after BC1 (DEF1) at 220 MeV and one at the end of the linac, in front of the spreader (DEF2), at 1.2 GeV. They are used, in conjunction with appropriate monitors, to measure the bunch length  $\sigma_z$  and the slice vertical and/or horizontal emittance in a dispersive free region. The betatron phase advance between the RF deflecting cavity and the monitor shall be  $\pi/2$ . The intrinsic resolution is  $\sim 15 \mu\text{m}$  for DEF1 and  $\sim 5 \mu\text{m}$  for DEF2.

The deflectors will operate in the S-band at a frequency of 2998.010 MHz. DEF1 is a rather short ( $\sim 0.5$  m) standing wave structure fed 5 MV by spilling RF power from an accelerating section modulator; it deflects the beam in the vertical direction only. DEF2 is a traveling wave structure,  $\sim 2$  m long, capable of 20 MV; it can deflect the beam in both the vertical and the horizontal direction.

The beta function at the deflectors,  $\beta_{dr}$  is 10 m at DEF1 and 20 m at DEF2.

### 11.3.13 Radiation Detectors

Radiation detectors ranging from diodes to pyrodetectors will be used, depending on the spectral distribution and intensity of the radiation, since the shorter the bunch the farther the emission spectrum extends towards high frequencies.

### 11.3.14 Bunch Arrival Time, Electro-Optical Sampling Station

The electro-optical effect exploits the birefringence induced in a suitable crystal by the transverse electric field produced by the beam relativistic electrons. For bunch charges of the order of 1 nC and at distances of a few millimetres the field can be of the order of tens of MV/m. Such a strong ultra fast changing electric field can be probed by a linearly polarized femtosecond laser pulse by detecting the laser phase delay induced by the birefringence in the crystal. The phase delay measurement is obtained by splitting the beam spatially in two opposite circular polarization components using a  $\lambda/4$  plate followed by a Wollaston prism; a balanced photo detector is then used to detect the difference of the two intensities,  $\Delta\text{EO}$ , proportional to  $\sin(\Gamma)$ , where  $\Gamma$  is the phase delay given by:

$$\Gamma = \left( \pi d / \lambda_0 \right) n_o^3 r_{41} E_a \sqrt{1 + 3 \cos^2 \alpha} \quad ,$$

and where  $\lambda_0$  is the laser central wavelength,  $d$  and  $n_o$  the EO crystal thickness and refractive index,  $r_{41}$  the electro-optical coefficient,  $E_a$  the electric field amplitude and  $\alpha$  the angle between the main crystallographic axes and the electric field.

Electro-optical sampling (EOS) has been used worldwide (FELIX, SPPS, TTF2) in recent years to non-

interceptingly measure the bunch arrival time in a single shot [12]. Furthermore, the technique is used to provide information on the electron bunch profile and the FEL pulse generation timing.

Each FERMI undulator chain will be equipped with an EOS station. The electron bunch duration at the end of the linac ranges from 700 to 1800 fs FWHM and the jitter of the bunch arrival time is 150 fs (rms) [13].

Using a time-to-space conversion scheme developed at SPPS [14] and probing the electro-optical crystal with sub-100 fs laser pulses the specified time resolution of  $\sim 100$  fs is reached, in a time window of  $\sim 10$  ps. A block diagram of an EOS station is shown in Figure 11.3.3; the station has four main components: laser, polarization diagnostics and delay line, in-vacuum setup, detection system.

All components, including the vacuum pipe, will be mounted on an optical table. To prevent vibrations the vacuum pipe will be connected to the rest of the machine through bellows.

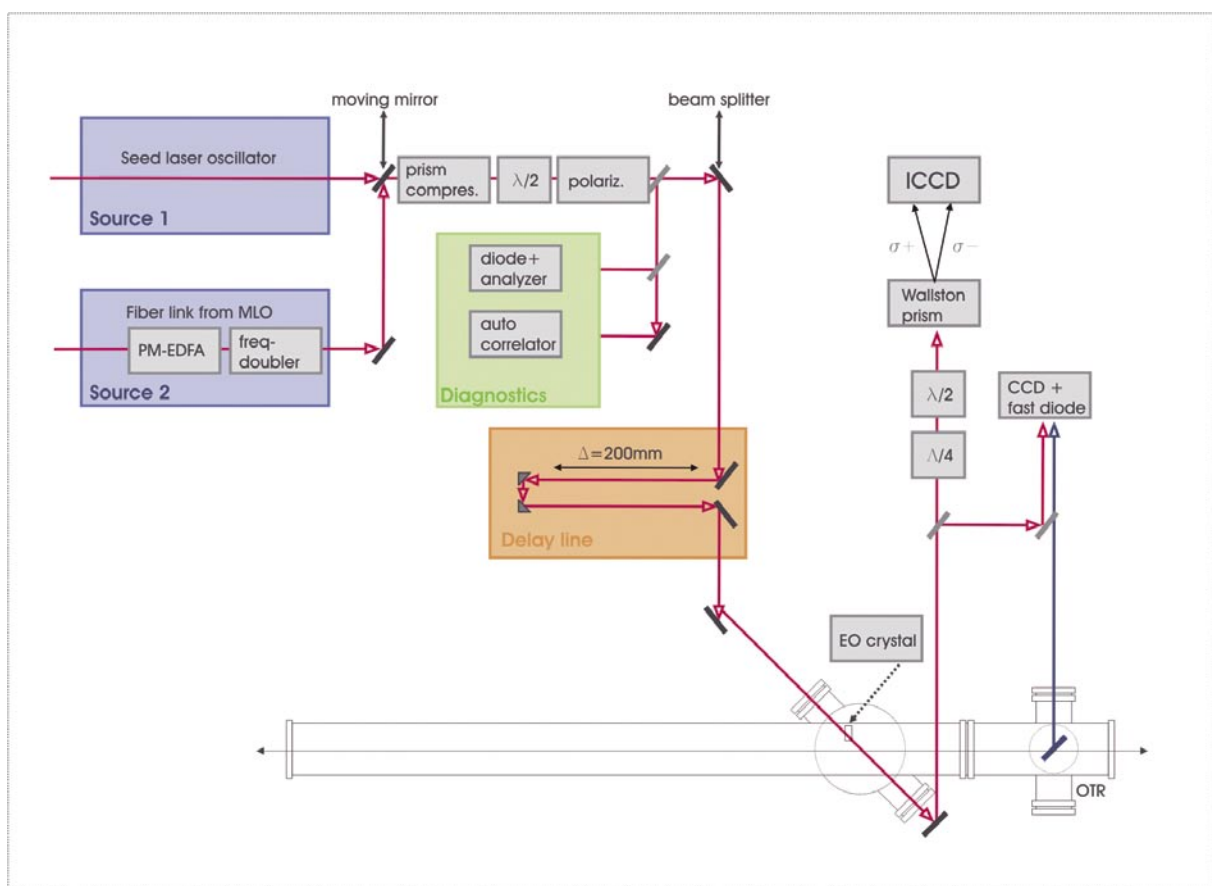


**Figure 11.3.3:**  
Electro Optical Sampling Station layout.

### 11.3.15 Bunch Phase Monitor

A non-intercepting, shot-to-shot bunch phase monitor (BPhM), first developed at DESY [15], is used to monitor the bunch arrival time. A compact and simple device, suited to be installed anywhere in the tunnel, it is based on an inductive, wide band (>10 GHz) RF ring pickup. It allows detecting the bunch centroid arrival time with respect to the *optical clock* pulse (see par. 9.3.2), but does not give information on bunch length. The measured bunch arrival time is obtained from the "average" phase of the pickup pulse response when excited by the electron bunch. The bandwidth of the pickup is in the GHz range.

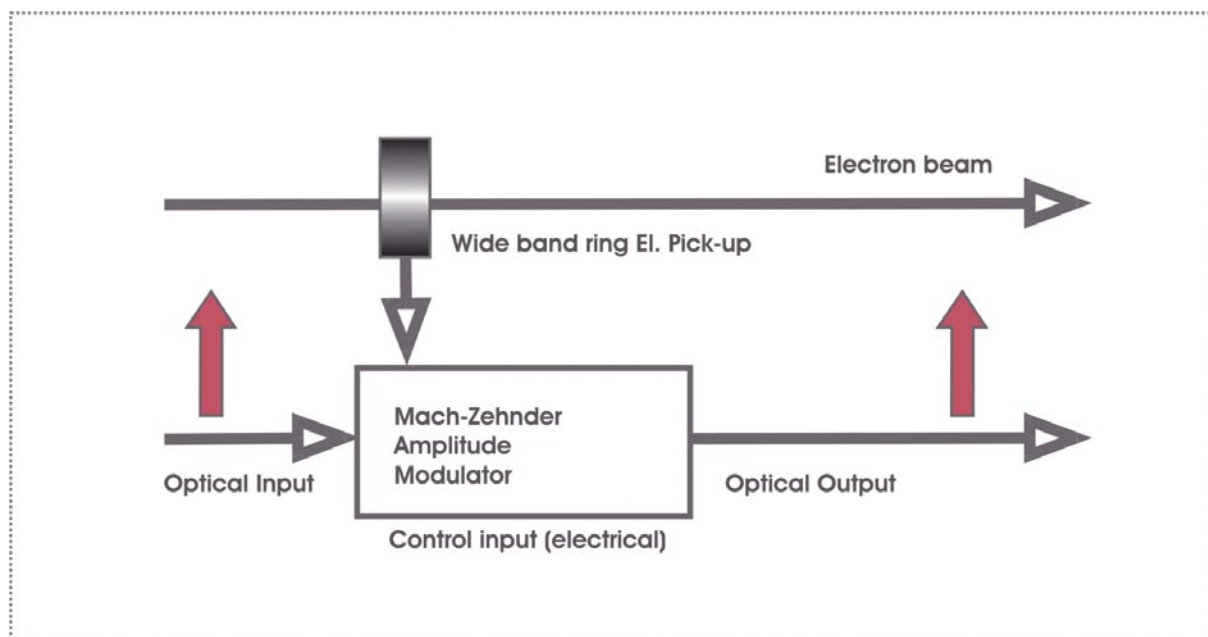


**Figure 11.3.4:**  
Bunch phase monitor block diagram.

The pickup RF signal zero-crossing, having a  $0.5\text{V/ps}$  slope, is sampled by a sub-ps laser pulse using a broadband electro-optical modulator (Mach-Zehnder interferometer). The modulator converts the bunch arrival time jitter into an amplitude modulation of the laser pulse which is then detected by a photo diode. Recent preliminary measurements show a time resolution of  $< 50\text{ fs}_{\text{RMS}}$ . In FERMI the laser pulse is provided via the ultra stable fibre timing distribution system whose time jitter is  $< 10\text{ fs}$ . A BPhM will be installed in front and behind both BC1 and BC2.

### 11.3.16 Bunch Length Monitor

To guarantee the performance of FEL1 and FEL2 in terms of output power long term stability, both the final average electron beam energy and the bunch peak current have to be stable. According to simulations, in order to guarantee the FEL beam specifications (see Par. 4.4 and 4.5), the current should be stable to within ( $\pm 5\%$ ) and ( $\pm 7\%$ ) for FEL1 and FEL2 respectively. From jitter studies - including



energy, R56 and X-band lineariser amplitude jitters, and ( $\pm 2\%$ ) bunch charge fluctuation - the relative bunch length variation needed to achieve a ( $\pm 5\%$ ) current stability is  $\delta\sigma_z / \sigma_z = (\pm 4.5\%)$ .

To meet the energy stability specification, given that the RF amplitude and phase seen by the beam cannot be measured accurately enough, energy and current have to be measured along the linac and the error signals fed back to the RF plant.

Error signals to stabilize the bunch current must be derived from both bunch charge and bunch length measurements. The charge is measured in the photoinjector using a toroid monitor and the bunch length using the monitors installed behind bunch compressor BC1 and BC2. Bunch length monitors, periodically calibrated using the RF deflectors installed downstream from BC1 and BC2, provide shot to shot, absolute bunch lengths.

Relative bunch length monitors are based on the detection of coherent synchrotron radiation (CSR) emitted in the last two bending magnets of the bunch compressor and coherent diffraction radiation (CDR) from two slits, one upstream and one downstream from each bunch compressor. Computations predict an energy per pulse of  $\sim 1 \mu\text{J}$  for CSR and of  $\sim 10 \mu\text{J}$  for CDR. The relative bunch length sensitivity is estimated of the order of 2% for both CSR and CDR. The use of two sources provides low cost redundancy and increased flexibility. Moreover, by normalizing the signal from the downstream CDR detector to that of the upstream one the measurement is made insensitive to charge fluctuations. Being both measurements non-intercepting, the bunch length can be measured in a single shot. For commissioning purposes only, CDR screen can also be used to produce CTR, allowing for easier, albeit intercepting, measurements. During commissioning, the RF phase of the upstream linac accelerating sections will be optimised for maximum compression using the CDR/CSR ratio. Once this is done, CSR and CDR signals will be used as error signal for the current stabilizing feedback loop.

### 11.3.17 Streak Camera

The streak camera provides single shot bunch length and bunch longitudinal profile measurements. The fastest commercially available streak camera (Hamamatsu FESCA 200) provides a time resolutions down to 200 fs rms (@  $\lambda=800$  nm). This value deteriorates at shorter wavelengths (800 fs rms @  $\lambda=250$  nm) due to the higher energy of the photons incident on the photo-cathode surface, leading to higher charge photo-electron bunches inside the streak tube. Furthermore, the streak camera is often used for measuring the relative time position of two optical pulses (up to a maximum of 10-20 ps separation). The camera time resolution is highest in the single sweep mode or at a low repetition rate ( $f_{\text{REP}} < 100$  Hz). This because, the time jitter of successive streaks being typically as high as 20 ps<sub>pk-pk</sub>, accumulation of several events rapidly spoils the resolution.

To achieve high repetition rate sweeps with sub ps jitter between them, a FESCA 200 single-sweep camera capable of operating in the synchro-scan dual sweep mode has been chosen, as the powerful diagnostic tool for the complete characterization of the photo-injector beam longitudinal characteristics. The bunch longitudinal profile is obtained illuminating the camera with the Cherenkov radiation produced by the beam in an aerogel cell [16]. The system can also be used to provide an accurate characterization of the 6-10 ps FWHM photo-cathode laser pulse.

### 11.3.18 Beam Loss Position Monitor Using Optical Fibres

To avoid vacuum breakdown and high radiation levels caused by electron losses a machine protection system is required. Beam loss issues for radioprotection and conventional radiation sensor systems are detailed in Chapter 15. An attractive alternative solution [17, 18] that allows real time monitoring of loss location and intensity is described in this Section.

Lost electrons, due to dark current, emittance growth or malfunction of the accelerator active components, hitting the vacuum chamber create a shower of secondary particles. A three dimensional reconstruction of the particle loss position can thus be obtained, within a few  $ns$ , using four radially arranged optical fibers, equidistant from the vacuum chamber axis: the shower hitting the fibers generates fast Cherenkov radiation signals detected by photomultipliers at the fiber ends, from which the shower position is reconstructed.

## 11.4 References

- [1] W. Graves *et al.*, PAC 2001, 2227 (2001).
- [2] J. Wu *et al.*, PAC2005, 1156 (2005).
- [3] R. Johnson *et al.*, PT13, DIPAC 2003, 193 (2003).
- [4] P. Craievich *et al.*, THPPH025, FEL '06 (2006).
- [5] M. Dehler, DIPAC 2005, 208 (2005).
- [6] V. Schlott *et al.*, EPAC 06, 3017 (2006).
- [7] K. Hacker *et al.*, EPAC 06, 1043 (2006).
- [8] <http://www.crytur.cz/main.php?id=11>.
- [9] H. Wiedemann, Particle Accelerator Physics, Vol. 1, Springer, 1999.
- [10] M. Zhang, Fermilab-TM-1988 (1996).
- [11] <http://www.bergoz.com/products/In-Flange.CT/In-Flange.CT.html>
- [12] A. Cavalieri *et al.* PRL, **94**, 114801 (2005).
- [13] P. Craievich, S. Di Mitri, Fermi Tech. Note ST/F-TN-05/26 (2005).
- [14] A. Cavalieri *et al.*, PRL **94**, 114801 (2005).
- [15] F. Loehl *et al.*, FLS 2006 ICFA workshop, May 2006, Desy.
- [16] J. Bähr *et al.*, DIPAC 2003 (2003).
- [17] M. Korfer *et al.*, DIPAC 2005, 299 (2005).
- [18] M. Korfer *et al.*, Nucl. Instr. and Methods A526, 537 (2004).

## Table of Contents

<b>11</b>	<b>Electron Beam Diagnostics</b>	321
11.1	Introduction	322
11.2	Measurements to be Performed	323
11.2.1	Injector Diagnostics	323
11.2.2	Laser Heater Diagnostics	324
11.2.3	Linac1, Linac2, Linac3 and Linac4	324
11.2.4	X-Band Linearizer	324
11.2.5	BC1 and BC2 Compressors Diagnostics	324
11.2.6	Front-end Last Diagnostics Station	325
11.2.7	End of Linac and Spreader Diagnostics	326
11.2.8	FEL Modulator Diagnostics	326
11.2.9	FEL Radiator Diagnostics	326
11.2.10	Beam Dump and FEL Downstream End Diagnostics	327
11.3	Instrumentation	327
11.3.1	Beam Position Monitors	327
11.3.2	Cavity Beam Position Monitor	327
11.3.3	Stripline Beam Position Monitors	328
11.3.4	Energy Beam Position Monitors	329
11.3.5	Scintillation Screens	329
11.3.6	Optical Transition Radiation (OTR) Screens	329
11.3.7	Emittance Measuring Devices	330
11.3.8	Intra-Undulator Pop-in Station	330
11.3.9	Wire-Scanners	331
11.3.10	Bunch Charge Measurement	331
11.3.11	Energy Spectrometers	331
11.3.12	Radio Frequency Deflectors	332
11.3.13	Radiation Detectors	332
11.3.14	Bunch Arrival Time, Electro-Optical Sampling Station	332
11.3.15	Bunch Phase Monitor	334
11.3.16	Bunch Length Monitor	334
11.3.17	Streak Camera	335
11.3.18	Beam Loss Position Monitor Using Optical Fibres	336
11.4	References	337